www.czasopisma.pan.pl PAN POLSKA AKADEMIA NAUK www.journals.pan.pl

Arch. Metall. Mater. **65** (2020), 3, 1045-1049

DOI: 10.24425/amm.2020.133215

YONG-HO KIM[1], IK-HYUN OH[1], HYO-SANG YOO[1], HYUN-KUK PARK[1], JUNG-HAN LEE[1], HYEON-TAEK SON[1*]

EFFECTS OF Si ADDITION ON MICROSTRUCTURE AND MECHANICAL PROPERTIES OF THE Al ALLOYS WITH HIGH Cr CONTENT PREPARED BY GAS ATOMIZATION AND SPS PROCESSES

This research describes effects of Si addition on microstructure and mechanical properties of the Al-Cr based alloys prepared manufactured using gas atomization and SPS (Spark Plasma Sintering) processes. The Al-Cr-Si bulks with high Cr and Si content were produced successfully using SPS sintering process without crack and obtained fully dense specimens close to nearly 100% T. D. (Theoretical Density). Microstructure of the as-atomized Al-Cr-Si alloys with high contents of Cr and Si was composed multi-phases with hard and thermally stable such as $Al_{13}Cr_4Si_4$, AlCrSi, Al_8Cr_5 and Cr_3Si intermetallic compounds. The average hardness values were 703 Hv for S5, 698 Hv for S10 and 824 Hv for S20 alloy. Enhancement of hardness value was resulted from the formation of the multi-intermetallic compound with hard and thermally stable and fine microstructure by the addition of high Cr and Si using rapid solidification and SPS process.

Keywords: Al-Cr-Si, Gas atomization, Spark plasma sintering, Powder, Rapid solidification

1. Introduction

Al-Si alloy systems have been considered attractive for automotive and aerospace application, due to light-weight, high specific strength, good wear resistance, high thermal stability, low thermal expansion coefficient and good creep resistance. On the other hand, hypereutectic Al-Si alloys with high Si content have been limited in their use as large primary Si phase and needle-like intermetallic compounds and segregation defects during casting [1-3]. Cr addition can improve the mechanical properties of Al alloy due to the grain refinement by preventing recrystallization and grain growth [4,5]. And Al-Cr alloy have been used as hard coating for cutting tool, mechanical and automotive components due to excellent wear resistance, thermal stability and oxidation resistance. However, brittle and coarse intermetallic compounds are formed during conventional casting processes of Al alloy with high Cr content. [6].

Powder metallurgy is one of important processes in order to overcome these problems, which is possible to obtain much better strength and surface characteristics than that of the conventional casting products due to the fine microstructure and excellent formability [7,8].

Generally, alloy powder with brittle intermetallic compounds are difficult to be consolidate by conventional forming processes due to low formability. Therefore, in this research, spark plasma sintering (SPS) process was applied. SPS process is characterized by high density consolidation in a short time. Low sintering temperature and short sintering time are expected to obtain fine microstructure and improvement of mechanical properties [9,10].

In recent, thermodynamic modeling of Al-Cr-Si alloy system has been reported [11,12], whereas, there are a few studies of the manufacturing process and characteristics of Al-Cr-Si alloy. In order to consolidation of the Al alloys with addition of high Cr and Si, gas atomization and spark plasma sintering process was applied in this study. Effects of Si addition on microstructure and mechanical properties of the gas-atomized and SPS sintered Al-Cr-Si alloy were investigated in this work.

2. Experimental

The Al-25Cr-5Si (S5, at.%), Al-30Cr-10Si (S10, at.%) and Al-30Cr-20Si (S20, at.%) alloys were prepared from pure Al, Si and Al-50Cr (wt.%) master alloy by using high frequency induction melting under vacuum. And theses alloy powders were manufactured using Ar gas atomizer process. The alloy ingots were melted and heated 1500°C under vacuum in an alumina

[1] KOREA INSTITUTE OF INDUSTRIAL TECHNOLOGY, 6 CHEOMDAN-GWAGIRO 208 BEON-GIL, BUL-GU, GWANGJU, 61012, REPUBLIC OF KOREA

* Corresponding author: sht50@kitech.re.kr

crucible. The melts were poured tundish with a melt deliver nozzle. A 4 mm diameter boron nitride atomizer orifice was used with an argon atomization pressure of 10 bar. The gas-atomized alloy powders were sieved under 200 μm by mechanical sieving machine. The sieved alloy powders were consolidated using spark plasma sintering (SPS) process within 600 ~ 1000°C under pressure 60 MPa in vacuum. During SPS sintering, the heating rate was 100°C/min. Microstructures of the gas-atomized powders and sintered alloys were analyzed using optical microscopy (OM), X-ray spectrometer (XRD), scanning electron microscopy (SEM) with energy-dispersive X-ray spectrometer (EDS), transmission electron microscopy (TEM) and image analyzer. Hardness of the SPS sintered alloys was measured using micro Vickers hardness tester with a load of 10 Kgf.

3. Results and discussion

Fig. 1 shows SEM images and particle size distributions of the as gas-atomized S5, S10 and S20 alloy powders with different Si contents. In all alloys, most of the powders were spherical morphology and smooth surfaces. Few large powders with several small powder aggregates and irregular shape were observed as shown in Fig. 1(a), (b) and (c). In Fig. 1(d), the average powder size distribution (D 50) of the as-atomized S5, S10 and S20 was 51, 53 and 55 μm, respectively. All alloy powders were similar particle size and morphology.

Cross-sectional SEM-BEI micrographs of the as-atomized S5, S10 and S20 alloy powders were shown in Fig. 2. As shown in Fig. 2(a), (b), (d) and (e)), microstructures of the S5 and S10

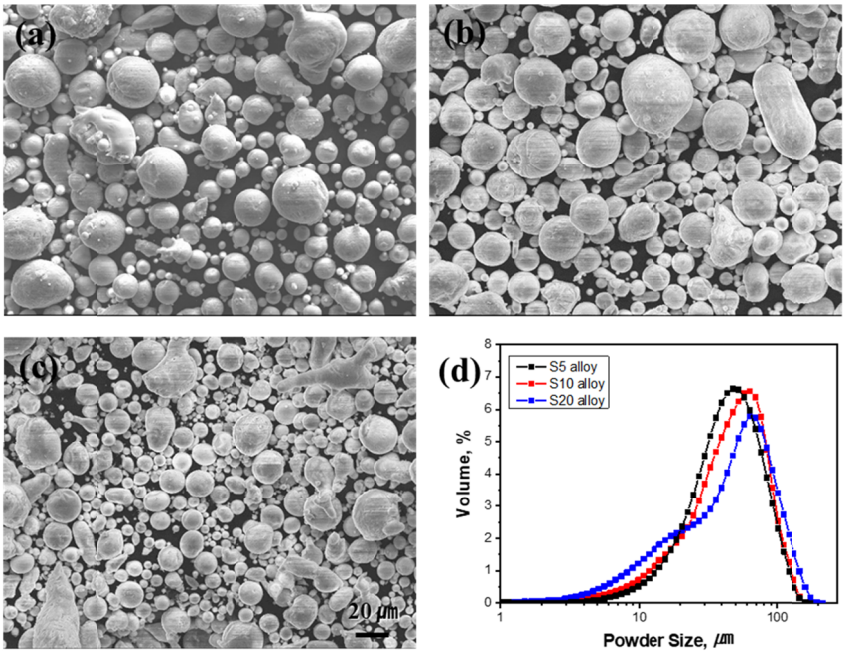

Fig. 1. SEM images and particle size distributions (d) of the as gas-atomized S5 (a), S10 (b) and S20 (c) alloy powders with different Si contents

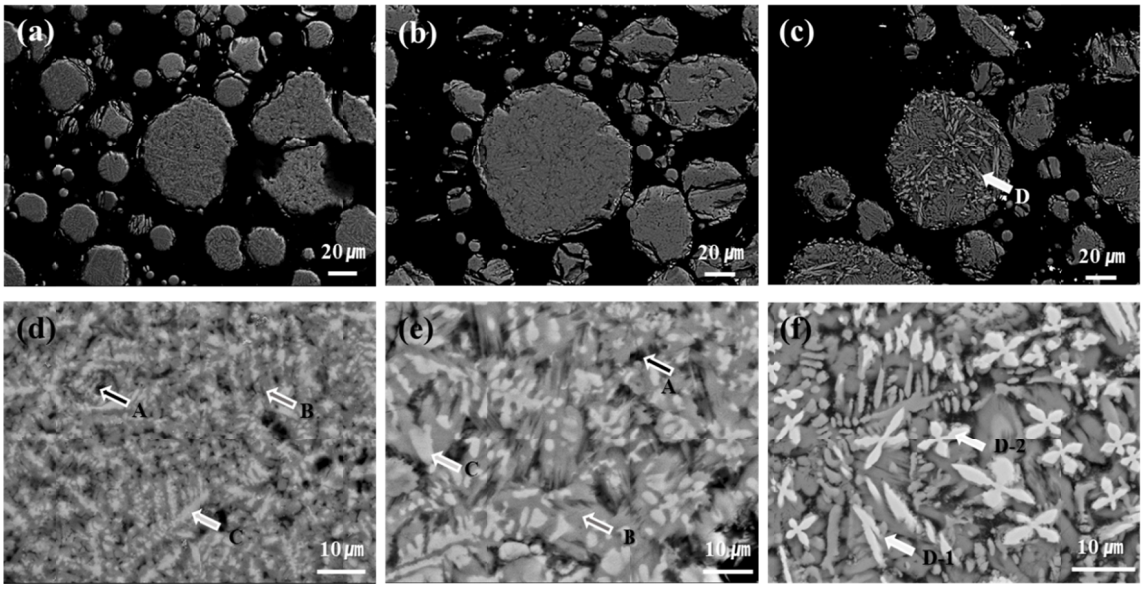

Fig. 2. Cross-sectional SEM-BEI micrographs of the as-atomized S5 ((a) and (d)), S10 ((b) and (e)) and S20 ((c) and (f)) alloy powders

alloy powders were composed of the phases with dark (marked as A), dark-grey (marked as B) and white-grey (marked as C) contrast. As Si content increased from 5 to 10%, size of intermetallic compounds with white grey contrast was increased slightly from 1.5 to 2.2 μm. On the other hand, microstructure of S20 alloy powder formed an additional intermetallic compound with white contrast dissimilar to that of the S5 and S10 alloy powders in Fig. 2(c) and (f). Intermetallic compounds with white contrast were observed two kinds of morphology as needle (marked as D-1) and radial (marked as D-2) as shown in Fig. 2(f). Average size of these intermetallic compound was approximately 11.5 μm.

Table 1 shows EDS element analysis of phases as marked A, B, C and D in the as-atomized S5, S10 and S20 alloy powder. As shown in Table 3, intermetallic compounds were mainly composed of Al, Cr and Si elements for the marked A and B, Al and Cr elements for the marked C and Cr and Si for the marked D, respectively. With increasing Si addition from 5 and 10 to 20%, Cr-Si rich intermetallic compounds were formed.

TABLE 1

EDS element analysis of phases as marked A, B, C and D in the as-atomized S5, S10 and S20 alloy powder

Element Mark	Al (at. %)	Cr (at. %)	Si (at. %)
A	81.30	14.02	4.68
B	68.86	19.36	11.78
C	65.52	29.64	4.84
D	4.87	57.54	37.59

In order to examine intermetallic compounds, XRD patterns of the as-atomized S5, S10 and S20 alloy powders were analyzed as shown Fig. 3. The as-atomized S5 and S10 alloy powders contained three major intermetallic compounds associated with $Al_{13}Cr_4Si_4$ (as marked A), AlCrSi (as marked B) and Al_8Cr_5 (as marked C). On the other hand, the as-atomized S20 alloy consisted of $Al_{13}Cr_4Si_4$, AlCrSi, Al_8Cr_5 and Cr3Si intermetallic compounds. Microstructure of the as-atomized Al-Cr-Si alloys with high contents of Cr and Si was composed multi-phases with hard and thermally stable.

Detailed analyses of the microstructure and the intermetallic compounds were carried out using TEM. Fig. 4 shows bright-field TEM, HR-TEM images and SAED patterns of the as-atomized Al-Cr-Si alloy powders. Analyses of TEM and SAED had distinguished that Cr-rich intermetallic compounds of Al_8Cr_5 and Cr_3Si had a cubic with a symbol group F-43m and cubic structure with a symbol group Pm-3n, respectively.

Fig. 5 demonstrated the area fraction of the intermetallic compounds for S5, S10 and S20 alloy powders with different Si contents obtained from image analysis. Area fraction of intermetallic phases in the S5 and S10 alloys was similar value. In the alloys with Si contents of 5 and 10%, area fraction of $Al_{13}Cr_4Si_4$, AlCrSi and Al8Cr5 was approximately 5, 76 and 19%, respectively in Fig. 5. As mentioned above, a new Cr3Si intermetallic compounds was formed by Si addition of 20%. Area fraction of $Al_{13}Cr_4Si_4$, AlCrSi, Al_8Cr_5 and Cr_3Si intermetallic compounds was approximately 7, 60, 21 and 12%, respectively.

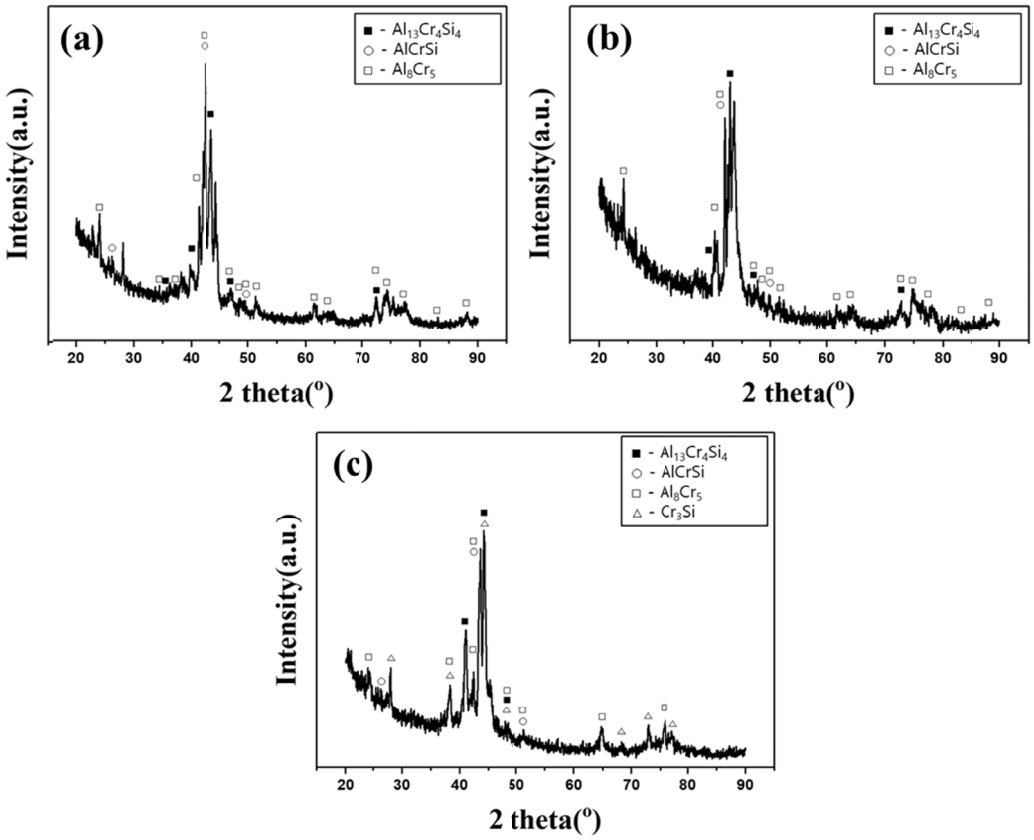

Fig. 3. XRD patterns of the as-atomized S5 (a), S10 (b) and S20 (c) alloy powders

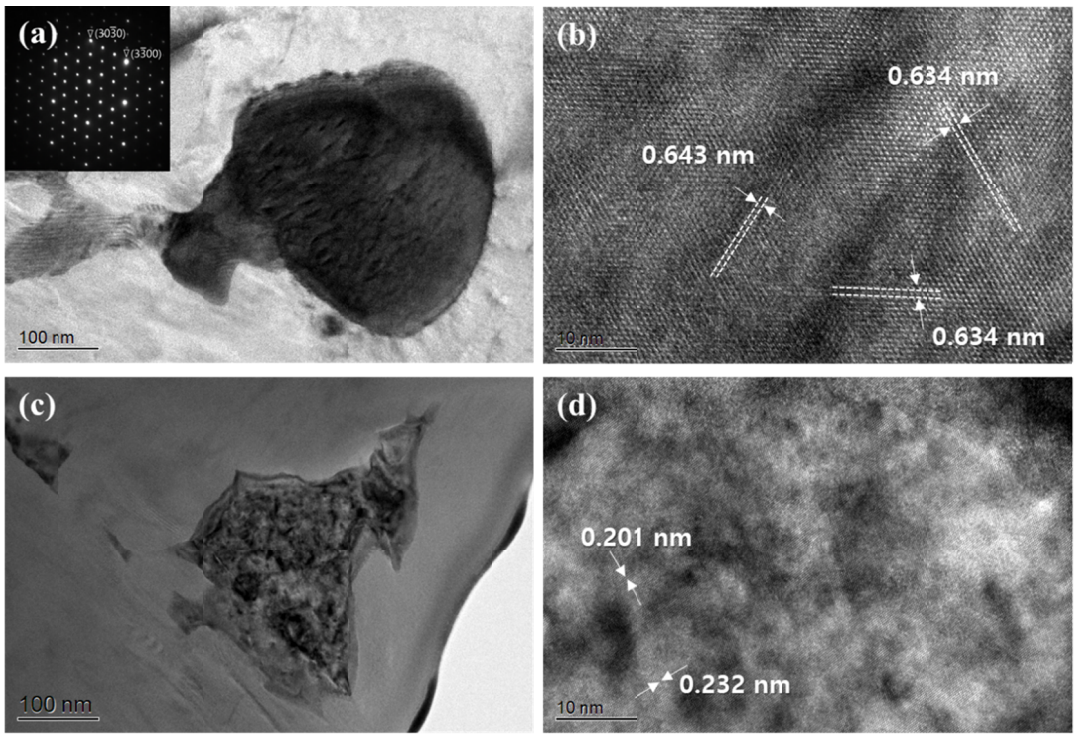

Fig. 4. The bright-field TEM images of the as-atomized Al-Cr-Si alloy powders; (a) and (b) Al8Cr5, (c) and (d) Cr3Si intermetallic compounds

With increasing Si content from 5and 10 to 20%, area fraction of the AlCrSi phase was decreased and Cr_3Si intermetallic compound was increased.

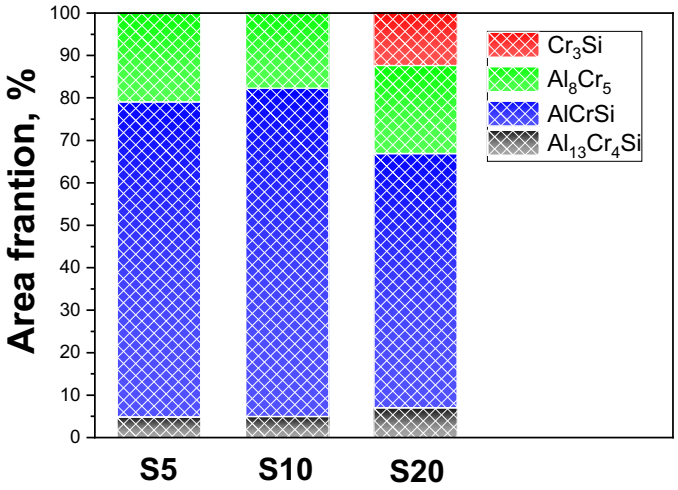

Fig. 5. Area fraction of the intermetallic compounds for S5, S10 and S20 alloy powders with different Si contents obtained from image analysis

The hardness of the SPS sintered S5, S10 and S20 alloys at 1000°C was measured by Vickers hardness tester as shown in Fig. 6. The average hardness values were 703 Hv for S5, 698 Hv for S10 and 824 Hv for S20 alloy. Hardness values of the SPS sintered S5, S10 and S20 alloys was much higher than that of the conventional high strength 7075 Al alloy. In particular, these values were higher or equal compared to that of light-weight high entropy alloys [13-15]. It is assumed that improvement of the hardness value was resulted from the formation of the multi-intermetallic compound with hard and thermally stable and fine microstructure by the addition of high Cr and Si using rapid solidification and SPS sintering process.

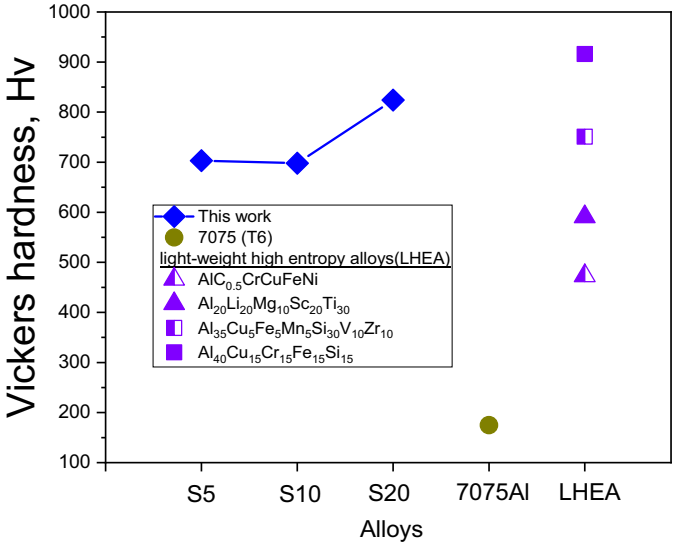

Fig. 6. The hardness of the SPS sintered S5, S10 and S20 alloys at 1000°C

4. Conclusions

In this research, effects of Si addition on microstructure and mechanical properties of the Al alloys with high Cr content prepared by gas atomization and SPS processes have been investigated. The Al-Cr-Si bulks with high Cr and Si content were produced successfully using SPS process without crack

and obtained fully dense specimens close to nearly 100% T. D. Microstructure of the as-atomized Al-Cr-Si alloys with high contents of Cr and Si was composed multi-phases with hard and thermally stable such as $Al_{13}Cr4Si_4$, AlCrSi, Al_8Cr_5 and Cr_3Si intermetallic compounds. The average hardness values were 703 Hv for S5, 698 Hv for S10 and 824 Hv for S20 alloy. Enhancement of hardness value was resulted from the formation of the multi-intermetallic compound with hard and thermally stable and fine microstructure by the addition of high Cr and Si using rapid solidification and SPS process.

Acknowledgments

Acknowledgments: This study has been conducted with the support of the Korea Institute of Industrial Technology (No. EO200004) and supported by 'Energy Efficiency & Resources Core Technology Program' of the Korea Institute of Energy Technology Evaluation and Planning (KETEP) granted financial resource from the Ministry of Trade, Industry & Energy, Republic of Korea. (No. 2018201010633B).

REFERENCES

[1] H.S. Kang, W.Y. Yoon, K.H. Kim, M.H. Kim, Y.P. Yoon, Mater. Sci. Eng. A **404**, 117 (2005).
[2] H.K. Feng, S.R. Yu, Y.L. Li, L.Y. Gong, J. Mater. Process. Tech. **208**, 330 (2008).
[3] L.G. Hou, H. Cui, Y.H. Cai, J.S. Zhang, Mater. Sci. Eng. A **527**, 85 (2009).
[4] S.P. Gupta, Mater. Character. **52**, 355 (2004).
[5] R.T. Li, Z.I. Dong, K.A. Khor, Scrip. Mater. **114**, 88 (2016).
[6] K.M. Chen, D.A. Tsai, H.C. Liao, In.G. Chen, J. Alloys Compd. **663**, 52 (2016).
[7] T.S. Kim, B.T. Lee, C.R. Lee, B.S. Chun, Mater. Sci. Eng. A **304-306**, 617 (2001).
[8] H.S. Kim, S.J. Hong, J. Alloys Compd. **586**, S428 (2014).
[9] L. Cao, W. Zeng, Y. Xie, J. Liang, D. Zhang, Mater. Sci. Eng. A **742**, 305 (2019).
[10] D. Guan, J. Gao, J. Sharp, W. Rainforth, J. Alloys Compd. **769**, 71 (2018).
[11] S. Cui, I.H. Jung, J. Alloys Compd. **708**, 887 (2017).
[12] Z. Zhou, Z. Li, X. Wang, Y. Liu, Y. Wu, M. Zhao, F. Yin, Thermch. Acta **577**, 59 (2014).
[13] C. Tung, J. Yeh, T. Shun, S. Chen, Y. Huang, H. Chen, Mater. Lett. **61**, 1 (2007).
[14] K. Youssef, A. Zaddach, C. Nju, D. Nju, C. Koch, Mater. Res. Lett. **3**, 95 (2014).
[15] J. Sanchez, I. Vicario, J. Albizuri, T. Guraya, J. Garcia, J. Mater. Res, Technol. **8**, 795 (2019).